Izumi, Tomoki; Kanaguchi, Takaaki; Fujihara, Masayuki

Numerical Investigation of Seaweed Expansion by Constructing Grounds on a Filled Sea Caldron

ICHE 2014, Hamburg - Lehfeldt & Kopmann (eds) - © 2014 Bundesanstalt für Wasserbau ISBN 978-3-939230-32-8

Numerical Investigation of Seaweed Expansion by Constructing Grounds on a Filled Sea Caldron

T. Izumi & T. Kanaguchi
Ehime University, Matsuyama, Japan

M. Fujihara
Kyoto University, Kyoto, Japan

ABSTRACT: Effects of a fishing ground newly constructed on a filled sea caldron in order to improve the environment of fishing grounds are numerically investigated in terms of the possibility for self-formation of seaweed beds. Tidal current simulations before and after filling up a caldron are firstly carried out by use of a multi-level density flow model. Then, *Sargassum horneri* being selected as a target species, the germlings released from the natural *Sargassum* bed are tracked based on the tidal current simulations by use of an Euler-Lagrangian transport model. From the results, the flow velocity get fast at the filled area after construction of fishing ground, and the germling particles cover approximately 60% of the filled area by three years under neglecting the survival ratio of germlings. Thus it is concluded that *Sargassum* bed would expand naturally on the filled area from year to year.

Keywords: Sargassum bed, Sea caldron, Tidal current simulation, Multi-level density flow model, Germling particles tracking, Euler-Lagrangian transport model

1 INTRODUCTION

The Seto Inland Sea is a representative semi-enclosed coastal sea in Japan, and consists of several basins which are connected by narrow channels or straits. Around channels or straits, there are many sea caldrons resulting from submarine erosion by tidal currents. In some of them, the accumulation of marine sediments worsen the environment of fishing grounds. For example, fishing activities such as the fixed net fishing may become difficult, and bottom water often becomes oxygen-deficient during summer when thermocline is dominant.

On the other hand, coastal area of the Seto Inland Sea is one of the most industrial areas in Japan. In the 1960s and early 1970s, land reclamation was intensively implemented to build many facilities for heavy industry. Consequently, more than half of the marine forest or seaweed bed that existed in the early 1960s has been lost (Takeoka, 2002). However, seaweed beds have high primary production capability and play a vital role in the aquatic ecosystems (Okuda, 2008). Thus it is very important to conserve seaweed beds.

One of the measures to improve such the environment is to construct seaweed bed by filling up the caldrons. In the present study, to assess a seaweed bed newly constructed on a filled caldron, tidal current is firstly numerically estimated using a multi-level density flow model. Then the possibility for the self-formation of seaweed beds (*Sargassum* beds) on the filled area is examined based on the estimated reach of the germlings which are released from the natural *Sargassum* bed and transported by the estimated tidal current, using the germling particles tracking method.

2 NUMERICAL MODELS

A multi-level density flow model and an Euler-Lagrangian transport model (Fujihara et al., 1997; Nakata et al., 2000) are employed for tidal current simulation and germling particles tracking, respectively.

2.1 *Tidal current simulation*

The multi-level density flow model consists of the momentum equation with *f*-plane and hydrostatic approximations, the continuity equation, the equation of free surface, the diffusion equations of water temperature and salinity, and the Knudsen's equation of state.

$$\frac{\partial \boldsymbol{u}}{\partial t}+\nabla_{\mathrm{h}}\cdot(\boldsymbol{u}\boldsymbol{u})+\frac{\partial(\boldsymbol{u}w)}{\partial z}+f\boldsymbol{k}\times\boldsymbol{u}=-\frac{1}{\rho}\nabla p+\nabla_{\mathrm{h}}\cdot(\nu_{\mathrm{h}}\nabla_{\mathrm{h}}\boldsymbol{u})+\frac{\partial}{\partial z}\left(\nu_{\mathrm{v}}\frac{\partial \boldsymbol{u}}{\partial z}\right) \tag{1}$$

$$\nabla_{\mathrm{h}}\cdot\boldsymbol{u}+\frac{\partial w}{\partial z}=0 \tag{2}$$

$$p=\int_z^{\eta}\rho g dz \tag{3}$$

$$\frac{\partial \eta}{\partial t}+\nabla_{\mathrm{h}}\cdot\int_{-H}^{\eta}\boldsymbol{u}dz=0 \tag{4}$$

$$\frac{\partial T}{\partial t}+\nabla_{\mathrm{h}}\cdot(\boldsymbol{u}T)+\frac{\partial(wT)}{\partial z}=\nabla_{\mathrm{h}}\cdot(K_{\mathrm{Th}}\nabla_{\mathrm{h}}T)+\frac{\partial}{\partial z}\left(K_{\mathrm{Tv}}\frac{\partial T}{\partial z}\right) \tag{5}$$

$$\frac{\partial Cl}{\partial t}+\nabla_{\mathrm{h}}\cdot(\boldsymbol{u}Cl)+\frac{\partial(wCl)}{\partial z}=\nabla_{\mathrm{h}}\cdot(K_{\mathrm{ch}}\nabla_{\mathrm{h}}Cl)+\frac{\partial}{\partial z}\left(K_{\mathrm{cv}}\frac{\partial Cl}{\partial z}\right) \tag{6}$$

$$\rho=\rho\left(T,Cl\right) \tag{7}$$

where $\boldsymbol{u}$ is the horizontally two-dimensional current vector, w the vertical current velocity, T the water temperature, Cl the salinity, ρ the water density, g the gravity acceleration, f the Coriolis parameter, η the free surface elevation from the mean sea level (positive upward), H the bottom depth from the mean sea level, ∇_{h} the horizontal differential operation, ν_{h} and ν_{v} the horizontal and vertical kinematic eddy viscosity coefficients, respectively, K_{Th} and K_{Tv} the horizontal and vertical turbulent diffusion coefficients of water temperature, respectively, K_{ch} and K_{cv} the horizontal and vertical turbulent diffusion coefficients of salinity, respectively, and $\boldsymbol{k}$ the unit vector (positive upward). The shear stress at the bottom is expressed as

$$\nu_{\mathrm{v}}\left.\frac{\partial \boldsymbol{u}}{\partial z}\right|_{z=-H}=\gamma^2\left|\boldsymbol{u}\right|\boldsymbol{u} \tag{8}$$

where γ^2 is the bottom friction coefficient.

These equations are discretized by the finite difference method on the staggered grids. In the discretization, the explicit time-marching scheme is employed for unsteady terms, the second-order upwind scheme for convection terms, and the central difference for diffusion terms.

2.2 *Germling particles tracking*

The Euler-Lagrangian transport model tracks particles of seaweed germlings which are transported in the flow fields computed by the above-mentioned flow model. The governing equations are as follows:

$$\frac{d\boldsymbol{X}}{dt}=\boldsymbol{V} \tag{9}$$

$$\boldsymbol{X}(0)=\boldsymbol{X}_0 \tag{10}$$

$$\boldsymbol{X}(n+1)^*=\boldsymbol{X}(n)+\boldsymbol{F}(n)\Delta t \tag{11}$$

$$\boldsymbol{X}(n+1)=\boldsymbol{X}(n)+\frac{\boldsymbol{F}(n)+\boldsymbol{F}(n+1)^*}{2}\Delta t \tag{12}$$

$$\boldsymbol{F}(n)=\boldsymbol{V}(n)+\left\{\left(\boldsymbol{V}(n)\cdot\nabla\right)\boldsymbol{V}(n)\right\}\Delta t \tag{13}$$

where $\boldsymbol{X}$ is the position vector, $\boldsymbol{V}$ the velocity vector in which settling velocity of germlings is taken into consideration, ∇ the differential operation, Δt the time increment; * denotes the temporary value at the time level, and n the time level. The initial value problem described in Eqs. (8) and (9) is solved using the two-step Runge-Kutta method described in Eqs. (10)-(12).

3 STUDY AREA AND COMPUTATIONAL CONDITIONS

The study area is located in the Seto Inland Sea, Japan, and the area with contour of water depth is shown in Figure 1. In the dotted frame, there is a sea caldron whose original maximum water depth is 27 m. An artificial seaweed bed will be constructed on the filled caldron. The caldron is filled up to 5 m below the mean sea surface. In the present study, change of tidal current before and after filling the caldron is numerically investigated and then the possibility for the self-formation of seaweed beds in and around filled area is estimated using the tidal current after filling the caldron.

The tidal current simulation is carried out for the domain of 10 km (east and west) × 6 km (north and south) including the artificial seaweed bed area. The whole domain is discretized into 50 m × 50 m square meshes horizontally and 10 levels vertically (2 m interval from depth of 0 m to 10 m, 4 m interval from depth of 10 m to 26 m, and deeper than 26 m as one layer). As open boundary conditions, the tidal current velocities are given at the west boundary and the free outflow condition is applied along the east boundary. Along the imaginary north boundary and land boundary, the non-slip condition is applied. The parameters used in the present study is summarized in Table 1. The coefficients of horizontal kinematic eddy viscosity and horizontal turbulent diffusion are determined according to Richardson's 4/3 law based on the computational grid. The coefficients of vertical kinematic eddy viscosity, vertical turbulent diffusion and bottom friction are determined to reproduce the observed tidal current.

The germling particles tracking is carried out using the results of tidal current simulation. Since the natural *Sargassum* beds consisting of the *Sargassum horneri* are found in the study area, the germling of the *Sargassum horneri* is selected as a target species. In the present study, one hundred particles representing the germling are equipped every computational grid where the natural *Sargassum* bed is formed, and released from the water surface of the grids to estimate the maximum reaching area. The settling velocity of the germling is based on Honda (2007). Since the *Sargassum horneri* is a yearly plant, the expansion of germling particles is considered by three years (the third generation) and evaluated in terms of "*the efficient area ratio*". In each generation, the particles are tracked until they settle the sea bottom. The ratio is defined as that of the settled area of the particles to the area artificially constructed. In the growth of germlings, survival ratio is assumed to be 100% because it has not been clear. The released timing of germlings has not also been known except during spring season. Thus four cases according to tidal time are considered as shown in Table 2.

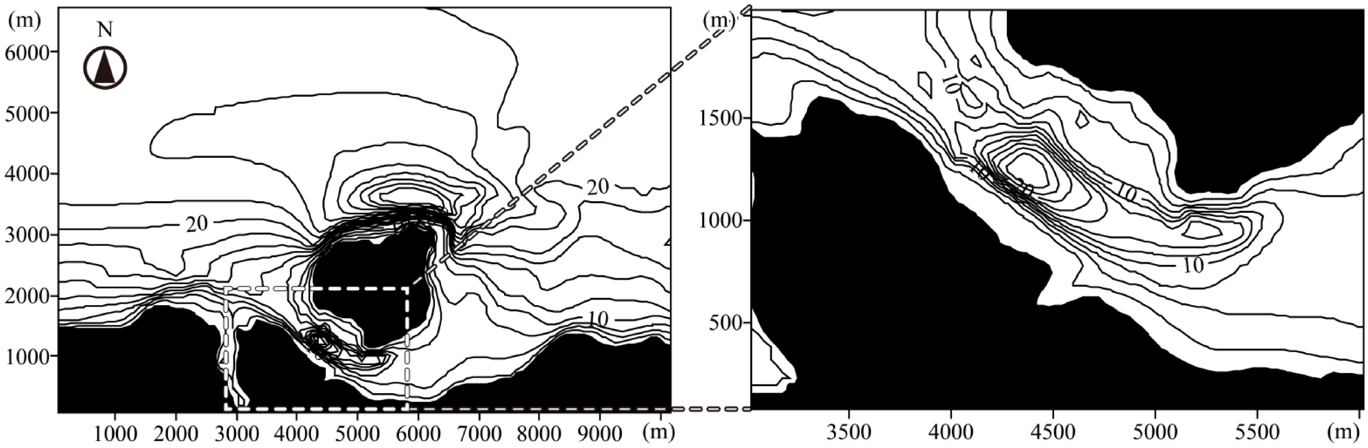

Figure 1. Study area.

Table 1. Parameters used in the present study.

Horizontal kinematic eddy viscosity coefficient, ν_h	1.0 m^2/s
Vertical kinematic eddy viscosity coefficient, ν_v	0.2 m^2/s
Horizontal turbulent diffusion coefficient, K_{Th}, K_{ch}	1.0 m^2/s
Vertical turbulent diffusion coefficient, K_{Tv}, K_{cv}	0.2 m^2/s
Bottom friction coefficient γ^2	0.0026

Table 2. Released timing of germlings.

Case 1	Spring tide	Flood tide with maximum velocity
Case 2	Spring tide	Ebb tide with maximum velocity
Case 3	Spring tide	Low tide
Case 4	Spring tide	High tide

4 RESULTS

4.1 *Change of tidal current*

Computed flow fields during four cases at 1 m deep before and after filling the caldron are shown through Figure 2 to 5.

As shown in Figure 2, the main flow direction is south-east at the flood tide. Difference of the flow velocities between two flow fields is found at the central part of the strait and the filled area. While the maximum flow velocity at the filled area before construction becomes approximately 53 cm/s, after construction becomes approximately 64 cm/s. Figure 3 shows that the main flow direction is north-west at the ebb tide. Difference of the flow fields is clearly found at the filled area; the maximum flow velocities at the filled area before and after construction are approximately 66 cm/s and 72 cm/s, respectively. In Figure 4 and 5, flow is very slow because of the slack water. Differences of before and after flow fields are thus invisible.

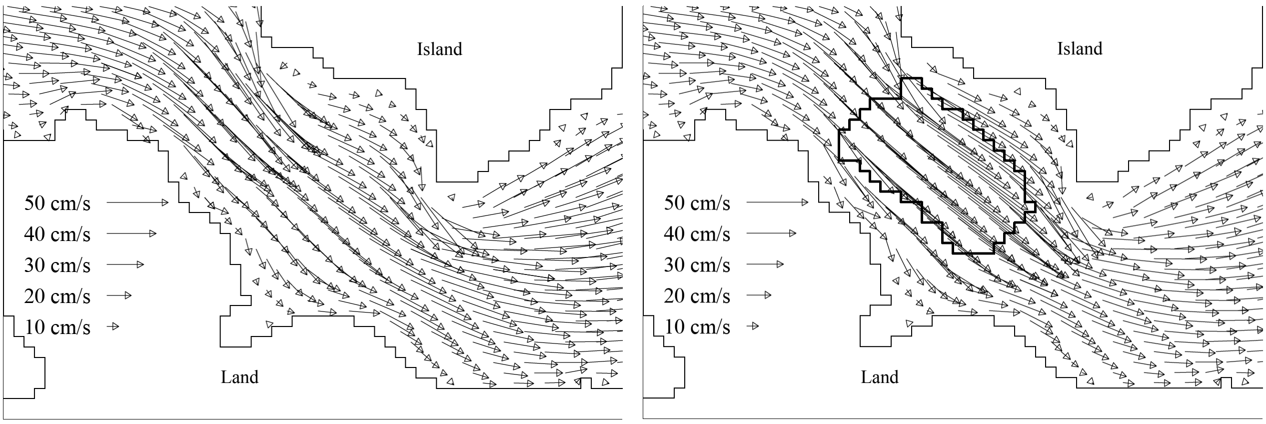

Figure 2. Computed flow fields before (left) and after (right) filling at maximum flood velocity (Case 1).

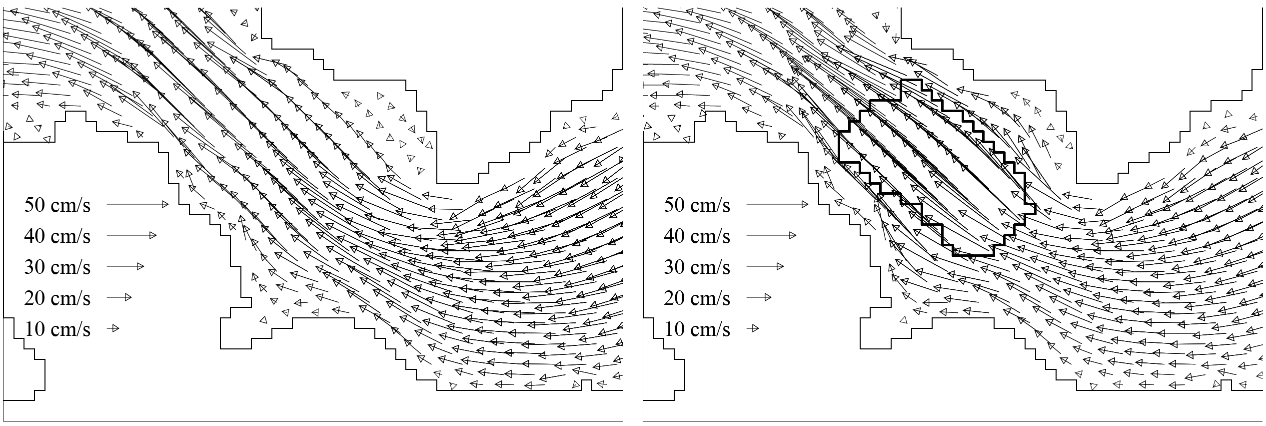

Figure 3. Computed flow fields before (left) and after (right) filling at maximum flood velocity (Case 2).

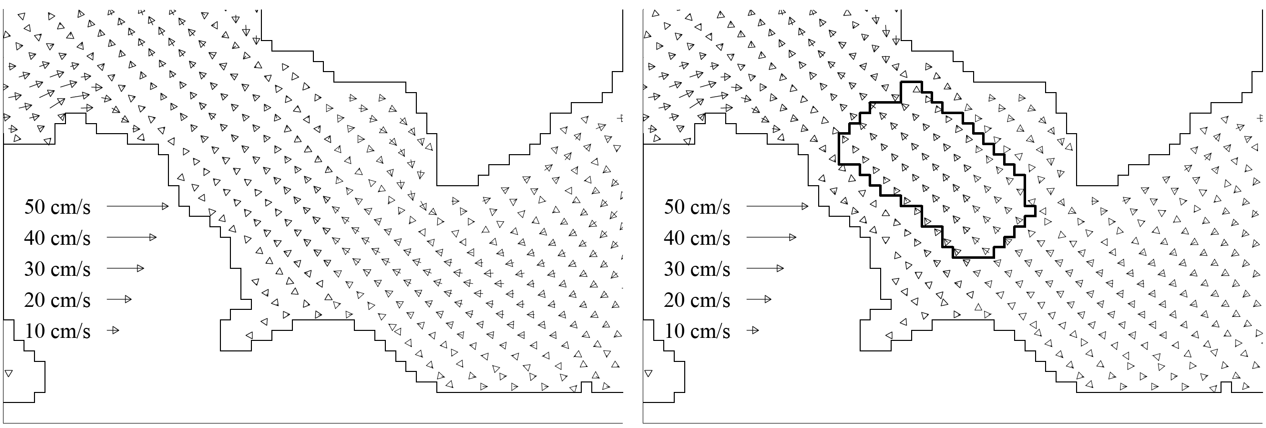

Figure 4. Computed flow fields before (left) and after (right) filling at low tide (Case 3).

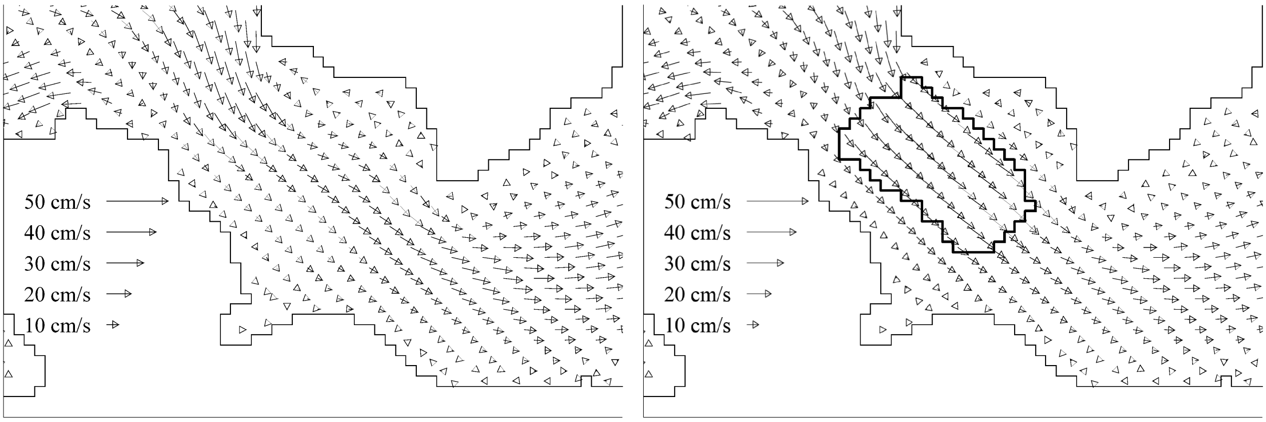

Figure 5. Computed flow fields before (left) and after (right) filling at high tide (Case 4).

4.2 *Germling particles tracking*

The initial position and reachable range of the germling particles every generation are shown through Figure 6 to 8. The reachable ranges represent the integrated results of germling particles tracking for all cases.

The results show that the germling particles in the first generation reach the north-east side of the filled area, and the germlings expand from generation to generation and then cover approximately 60% of the filled area by three years. Thus it is concluded that the *Sargassum* bed would expand naturally from year to year and be formed on the filled area.

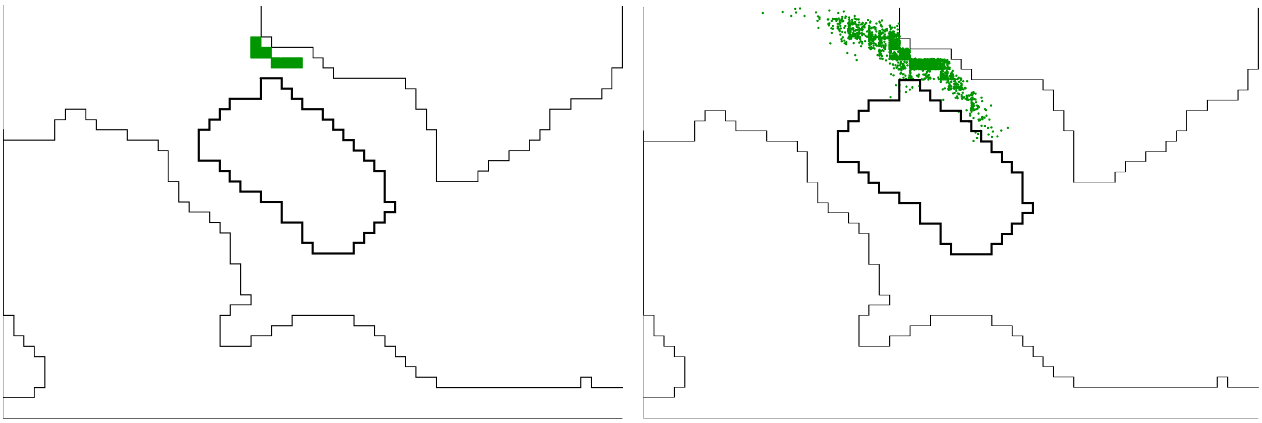

Figure 6. Initial position (left) and reachable range of germling particles (right) in the first generation.

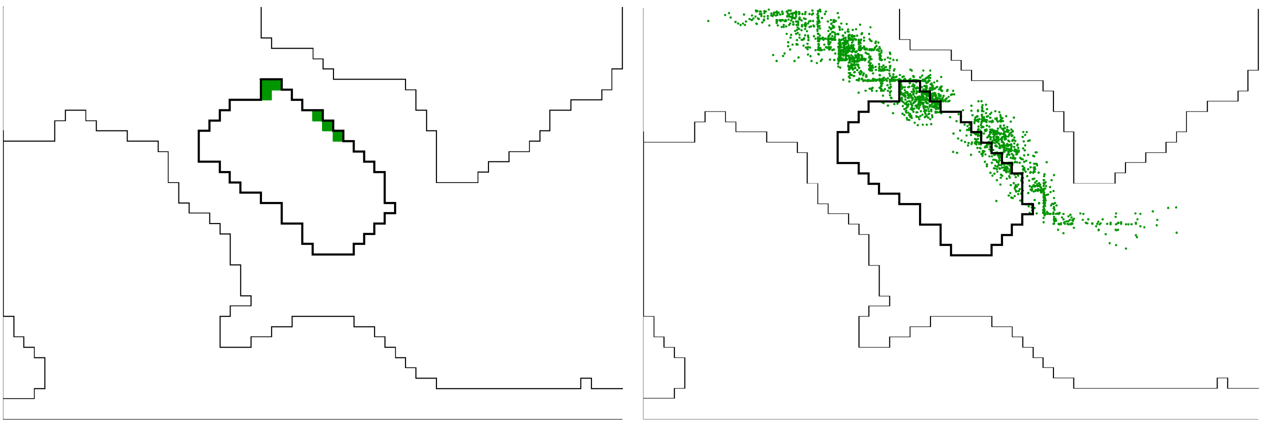

Figure 7. Initial position (left) and reachable range of germling particles (right) in the second generation.

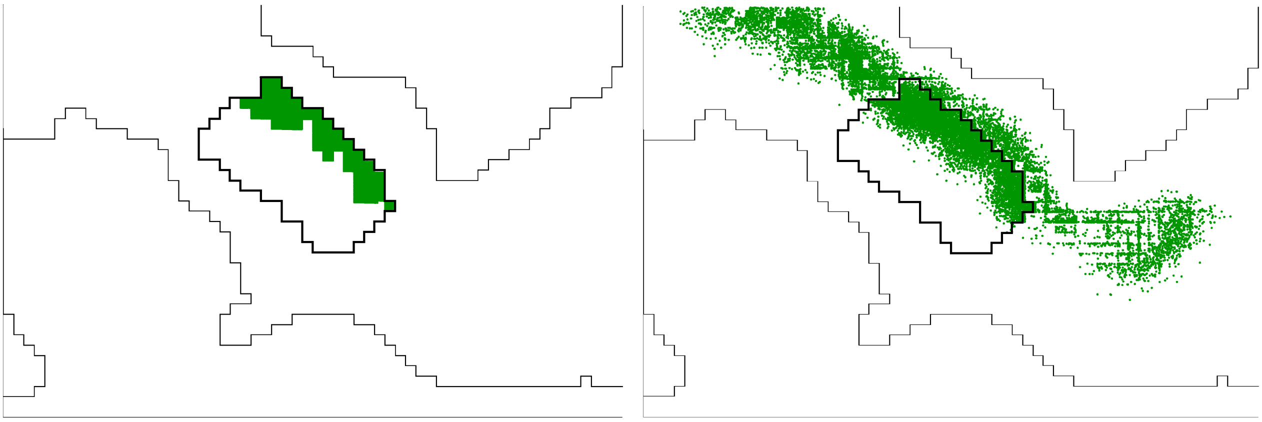

Figure 8. Initial position (left) and reachable range of germling particles (right) in the third generation.

5 CONCLUSIONS

In order to assess the seaweed bed artificially constructed by filling a sea caldron, change of tidal current and the expansion of the seaweed bed from the naturally existing area are numerically examined.

The results show that the changes of tidal current appear at the central part of the strait and the filled area, and that the seaweed bed (*Sargassum* bed) would expand from year to year and be formed on the filled area.

NOTATION

$\boldsymbol{u}$	horizontally two-dimensional current velocity vector
w	vertical current velocity
T	water temperature
Cl	salinity
ρ	water density
g	gravity acceleration
f	Coriolis parameter
η	elevation from the mean sea level (positive up ward)
H	water depth
∇_h	horizontal differential operation
ν_h	horizontal kinematic eddy viscosity coefficient
ν_v	vertical kinematic eddy viscosity coefficient
K_{Th}	horizontal turbulent diffusion coefficient of water temperature
K_{Tv}	vertical turbulent diffusion coefficient of water temperature
K_{ch}	horizontal turbulent diffusion coefficient of salinity
K_{cv}	vertical turbulent diffusion coefficient of salinity
$\boldsymbol{k}$	unit vector (positive upward)
$\boldsymbol{X}$	position
$\boldsymbol{V}$	velocity including settling velocity of germlings
∇	differential operation
Δt	time increment
n	time level

REFERENCES

Fujihara, M., Suenaga, Y., Nakarta, H., Nagasawa, T., Yamada, H. (1997). Numerical simulation on the transport of brown sole eggs and larvae using an Euler-Lagrangian method. Fisheries Engineering, Vol. 34, No. 2, pp. 147-154. (in Japanese with English abstract)

Honda, M. (2007). Settlement of germlings in some Japanese Sargassaceae. Sessile Organisms, Vol. 24, No. 2, pp. 89-94. (in Japanese with English abstract)

Nakata, H., Fujihara, M., Suenaga, Y., Nagasawa, T., Fujii, T. (2000). Effect of blows on the transport and settlement of brown sole (Pleuronectes herzensteini) larvae in a shelf region of the Sea of Japan: numerical experiments with an Euler-Lagrangian model. Journal of Sea Research, Vol. 44, pp. 91-100.

Okuda, K. (2008). Coastal environment and seaweed-bed ecology in Japan. Kuroshio Science, Vol. 2, No. 1, pp. 15-20.

Takeoka, H. (2002). Progress in Seto Inland Sea research. Journal of Oceanography, Vol.58, pp. 93-107.